



JID Open

β -Catenin Stabilization in Skin Fibroblasts Causes Fibrotic Lesions by Preventing Adipocyte Differentiation of the Reticular Dermis

Maria Mastrogiannaki^{1,2,3}, Beate M. Lichtenberger^{1,2,3}, Andreas Reimer¹, Charlotte A. Collins², Ryan R. Driskell¹ and Fiona M. Watt¹

The Wnt/ β -catenin pathway plays a central role in epidermal homeostasis and regeneration, but how it affects fibroblast fate decisions is unknown. We investigated the effect of targeted β -catenin stabilization in dermal fibroblasts. Comparative gene expression profiling of stem cell antigen 1⁻ (Sca1⁻) and Sca1⁺ neonatal fibroblasts from upper and lower dermis, respectively, confirmed that Sca1⁺ cells had a preadipocyte signature and showed differential expression of Wnt/ β -catenin-associated genes. By targeting all fibroblasts or selectively targeting Dlk1⁺ lower dermal fibroblasts, we found that β -catenin stabilization between developmental stages E16.5 and P2 resulted in a reduction in the dermal adipocyte layer with a corresponding increase in dermal fibrosis and an altered hair cycle. The fibrotic phenotype correlated with a reduction in the potential of Sca1⁺ fibroblasts to undergo adipogenic differentiation *ex vivo*. Our findings indicate that Wnt/ β -catenin signaling controls adipogenic cell fate within the lower dermis, which potentially contributes to the pathogenesis of fibrotic skin diseases.

Journal of Investigative Dermatology (2016) **136**, 1130–1142; doi:10.1016/j.jid.2016.01.036

INTRODUCTION

The epidermis is maintained by distinct subpopulations of stem cells whose fate is regulated by intrinsic mechanisms and external signals from the niche (Kretzschmar and Watt, 2014; Lim and Nusse, 2013). Signaling between epidermal stem cells and cells in the underlying dermis is reciprocal (Millar, 2002; Sennett and Rendl, 2012). Such interactions can occur at close range—for example, via extracellular matrix (ECM) deposition (Fujiwara et al., 2011)—and by long-range signaling mediated by epidermal secreted factors (Collins et al., 2011; Donati et al., 2014). Furthermore, factors secreted by proliferating adipocyte progenitors (Festa et al., 2011) and differentiated adipocytes (Plikus and Chuong, 2014; Plikus et al., 2008) regulate the hair growth cycle.

The dermis contains a variety of subpopulations of mesenchymal cells with different locations and functions (Driskell and Watt, 2015). At the E12.5 stage of embryonic

development, mouse dermal cells are capable of differentiating into all the different fibroblast types present in postnatal skin. However, at about E16.5, the dermal mesenchyme undergoes commitment to two different lineages. In late embryonic and neonatal skin, the upper dermal lineage gives rise to papillary fibroblasts, the cells of the arrector pili muscle (responsible for piloerection), the dermal sheath, and the dermal papilla (DP). The lower dermal lineage gives rise to the reticular fibroblasts, which deposit most of the skin fibrillar collagen, preadipocytes and mature adipocytes (Driskell et al., 2013). The different fibroblast lineages are functionally significant, because the upper papillary lineage is required for new hair follicle (HF) formation, and the lower (or reticular) lineage is responsible for the first wave of dermal repair after wounding (Driskell et al., 2013). However, the molecular mechanisms that determine fibroblast fate decisions are largely uncharacterized (Driskell et al., 2009).

Epidermal Wnt/ β -catenin signaling causes profound changes in the underlying dermis, leading to expansion of both the upper and lower dermal lineages, *de novo* formation of DPs, and an increase in adipocyte differentiation (Collins et al., 2011; Donati et al., 2014; Lichtenberger et al., 2016). In addition, there is compelling evidence that Wnt/ β -catenin signaling in fibroblasts regulates the composition of the dermis. β -Catenin is necessary and sufficient to specify dermal fate in different body regions during mouse embryonic development (Atit et al., 2006; Ohtola et al., 2008). Wnt/ β -catenin signaling has a well-characterized inhibitory effect on adipogenic differentiation (Gesta et al., 2007; Kennell and MacDougald, 2005; Longo et al., 2004) and is required in the DP to promote HF formation and control DP activity and size (Enshell-Seiffers et al., 2010; Kaushal et al., 2015; Tsai et al., 2014).

¹Centre for Stem Cells and Regenerative Medicine, King's College London, Guy's Hospital, Great Maze Pond, London SE1 9RT, UK; and ²Wellcome Trust Centre for Stem Cell Research, University of Cambridge, Tennis Court Road, Cambridge CB2 1QR, UK

³These authors contributed equally to this work.

Correspondence: Fiona M. Watt, Centre for Stem Cells and Regenerative Medicine, King's College London, Floor 28, Tower Wing, Guy's Hospital, Great Maze Pond, London SE1 9RT, UK. E-mail: fiona.watt@kcl.ac.uk

Abbreviations: DAPI, 4', 6-diamidino-2-phenylindole; DP, dermal papilla; ECM, extracellular matrix; EGFP, enhanced green fluorescent protein; HF, hair follicle; PDGFR α , platelet-derived growth factor receptor α ; Sca1, stem cell antigen 1

Received 23 September 2015; revised 13 January 2016; accepted 28 January 2016; accepted manuscript published online 20 February 2016; corrected proof published online 7 April 2016

Furthermore, it was shown recently that expression of stabilized β -catenin in the fibroblasts of mouse ventral dermis at E16.5 results in progressive skin fibrosis, with thickened collagen fibers and altered collagen fibril morphology (Hamburg-Shields et al., 2015).

In this study, we performed comparative gene expression profiling of distinct populations of neonatal fibroblasts, which showed differential expression of Wnt pathway genes. Using a conditional targeting approach, we examined the effects of β -catenin stabilization in all fibroblasts or selectively in reticular fibroblasts. Our findings indicate a key role of Wnt/ β -catenin signaling in regulating the differentiation of reticular fibroblasts into adipocytes.

RESULTS

Differential expression of adipocyte genes in upper and lower dermal fibroblasts

As previously reported (Collins et al., 2011), in *Pdgfra*EGFP mice (Hamilton et al., 2003) enhanced green fluorescent

protein (EGFP) expressed under the control of the platelet-derived growth factor receptor α (*Pdgfra*) promoter is detected in nuclei of all dorsal skin fibroblasts (Figure 1a–d). In neonatal (P2) skin, stem cell antigen 1 (*Sca1*) is absent from the upper (papillary) dermis but is expressed by reticular fibroblasts, preadipocytes, and skin adipocytes in the lower dermis (Donati et al., 2014; Driskell et al., 2013; Festa et al., 2011). Immunolabeling confirmed that most reticular fibroblasts express *Sca1* at P2 (Figure 1c and d). We have previously shown that fibroblasts that express the protein Delta homolog 1 (*Dlk1*) at E16.5 give rise to the *Sca1*⁺ fibroblasts and mature adipocytes present in P2 and adult skin, although *Dlk1* is no longer expressed in adult skin (Driskell et al., 2013; Lichtenberger et al., 2016). To compare fibroblasts from the upper and lower dermis, we sorted EGFP⁺ cells from P2 dorsal dermis and fractionated the cells further on the basis of *Sca1* surface marker expression (Figure 1e). We also sorted EGFP⁺/*Sca1*⁺ cells as a control.

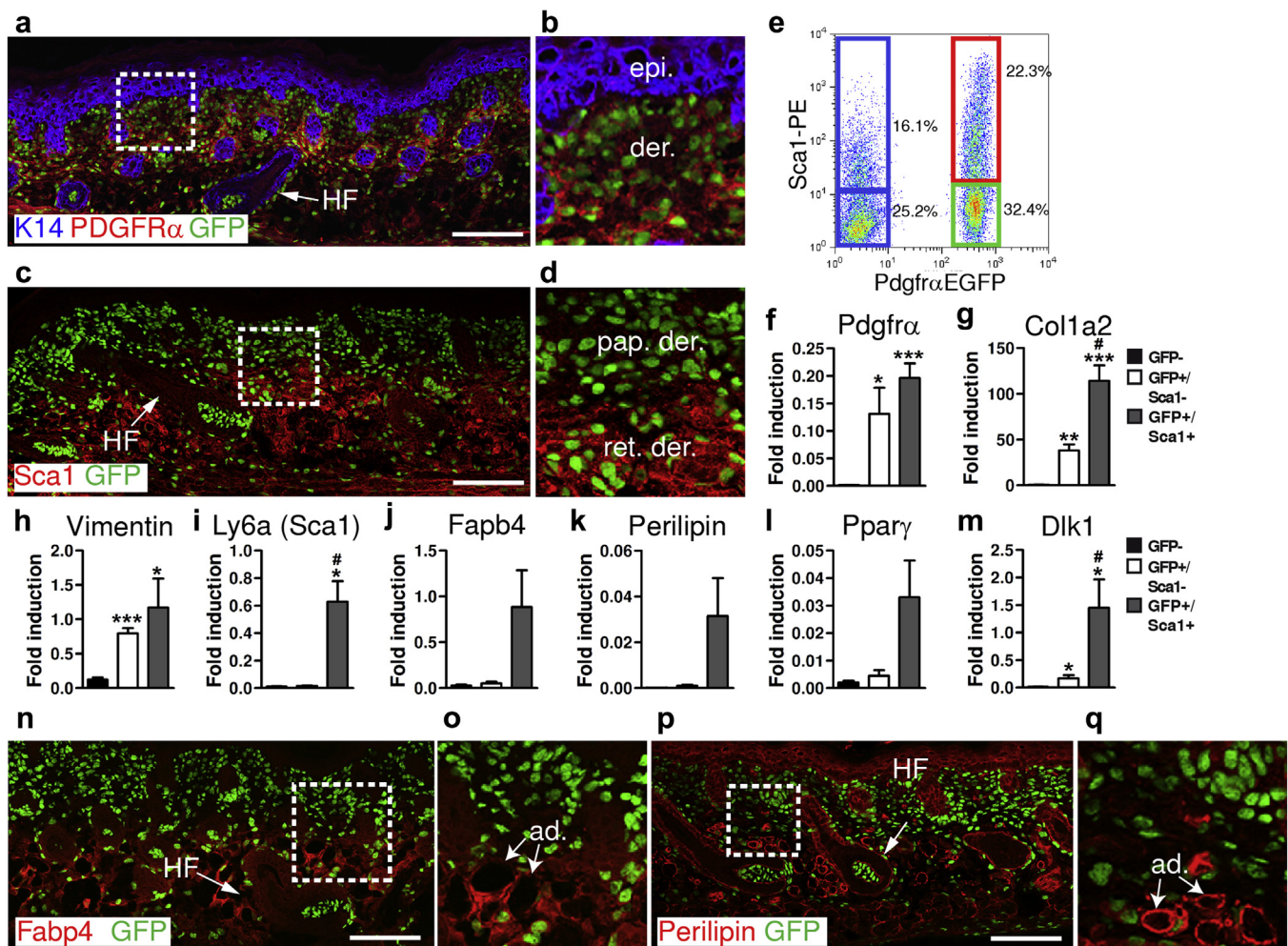


Figure 1. Localization and isolation of *Sca1*⁺ and *Sca1*⁻ dermal fibroblasts. (a–d, n–q) Sections of P2 back skin from *Pdgfra*EGFP mice showing expression of nuclear EGFP and immunostaining for (a, b) K14 and PDGFR α , (c, d) *Sca1*, (n, o) *Fabp4*, and (p, q) *Perilipin*. (b, d, o, q) are enlargements of selected regions of (a, c, n, p), respectively. Scale bars = 150 μ m. (e) Flow cytometry plot showing gating of different dermal subpopulations on the basis of *Pdgfra*EGFP and *Sca1* expression. (f–m) Quantitative real-time PCR analysis of mRNA levels in sorted cell populations: *Pdgfra*EGFP/*Sca1*⁻, *Pdgfra*EGFP⁺/*Sca1*⁻ and *Pdgfra*EGFP⁺/*Sca1*⁺. Genes were normalized to the *Gapdh* gene. Error bars represent standard error of the mean of replicates from four mice. * $P \leq 0.05$, ** $P \leq 0.005$, *** $P \leq 0.0005$ compared with GFP⁻ cells; # $p \leq 0.05$ compared with EGFP⁺/*Sca1*⁻ cells. ad, adipocyte; epi, epidermis; der, dermis; EGFP, enhanced green fluorescent protein; GFP, green fluorescent protein; HF, hair follicle; pap, papillary; PDGFR α , platelet-derived growth factor receptor α ; ret, reticular.

Quantitative real-time PCR (QPCR) analysis of mRNA isolated from the different dermal subpopulations showed that mRNAs corresponding to *Pdgfra* and the fibroblast marker genes *Col1a2* and *Vimentin* were highly enriched in both $Pdgfra^+$ subpopulations relative to $Pdgfra^-$ cells (Figure 1f–h), whereas mRNA corresponding to *Ly6a* (*Sca1*) was highly enriched in the $Pdgfra^+/Sca1^+$ fraction (Figure 1i), confirming the relative purity of the sorted cell populations. The adipocyte/preadipocyte marker genes *Fabp4*, *Perilipin*, *Pparg*, and *Dlk1* were also enriched in $Pdgfra^+/Sca1^+$ cells, consistent with previous reports (Driskell et al., 2013; Festa et al., 2011) (Figure 1j–m). The QPCR results were confirmed by immunofluorescence labeling of P2 dorsal skin with antibodies to *Fabp4* and *Perilipin* (Figure 1n–q).

Differential expression of Wnt pathway genes in upper and lower dermal fibroblasts

To explore the differences between $Pdgfra^+/Sca1^+$ and $Pdgfra^+/Sca1^-$ fibroblasts, we carried out gene expression profiling using RNA from flow-sorted cells. We found that 1,457 entities were regulated by more than 2-fold (*t* test, $P < 0.05$) (Figure 2a; see Supplementary Table S1 online), showing that global differences in gene expression distinguish the two fibroblast subpopulations. In addition to differential expression of adipogenic genes, there was differential expression of genes encoding zinc finger proteins (Gupta et al., 2012) and regulators of the Wnt, BMP, Notch, and PDGF signaling pathways (Figure 2b and c).

Because Wnt/ β -catenin signaling is known to regulate dermal development, the differential expression of genes associated with this pathway was of particular interest (Figure 2c). Several Wnt/ β -catenin pathway genes were differentially regulated in $Pdgfra^+/Sca1^+$ and $Pdgfra^+/Sca1^-$ fibroblasts, which we confirmed by QPCR in independent biological samples (Figure 2d–j). $Pdgfra^+/Sca1^+$ fibroblasts expressed significantly lower levels of *Wnt5a* ligand, the Wnt receptor *Frzb*, and the Wnt effector *Lef1*, as well as several other Wnt pathway genes including *Axin2* and *Dkk1* (Figure 2d–h; see also Driskell et al., 2013). However, $Sca1^+$ cells expressed significantly higher levels of the Wnt receptor *Fzd4* and the Wnt effector *Tcf7l2* (Figure 2i and j). *Tcf7l2*, commonly known as *Tcf4*, is expressed in human adipose tissue, and gene variants are associated with susceptibility to Type 2 diabetes and inability to lose weight after lifestyle interventions (Cauchi et al., 2006; Haupt et al., 2010). There was no significant difference in β -catenin mRNA levels in $Pdgfra^+/Sca1^-$ and $Pdgfra^+/Sca1^+$ fibroblasts at P2 (Figure 2k). However, immunostaining showed differential protein expression of β -catenin in the upper and lower dermis of neonatal skin, with high levels of nuclear β -catenin in papillary fibroblasts and only few nuclear β -catenin–positive cells within the adipose tissue (Figure 2l–p).

Consistent with the microarray and QPCR data, immunostaining of neonatal skin with antibodies recognizing *Tcf3/4* and *Lef1* showed that *Tcf3/4* localized to the lower reticular dermis ($Pdgfra^+/Sca1^+$), whereas *Lef1* stained the upper papillary dermis ($Pdgfra^+/Sca1^-$) (Figure 2n, q, and r). However, there were some scattered cells in the lower

dermis that coexpressed *Tcf3/4* and *Lef1* (Figure 2n, white arrowheads).

We conclude that neonatal dermis is compartmentalized such that Wnt/ β -catenin signaling pathway components are differentially expressed in $Sca1^+$ and $Sca1^-$ fibroblasts.

Constitutive β -catenin stabilization in postnatal skin fibroblasts reduces the adipocyte layer and disturbs the hair growth cycle

Given the inhibitory effect of Wnt/ β -catenin signaling on adipogenic differentiation (Gesta et al., 2007; Kennell and MacDougald, 2005; Longo et al., 2004), we speculated that activating the pathway in postnatal skin fibroblasts would change the composition of the dermis by altering neonatal fibroblast lineages or differentiation. To determine the effect of active Wnt/ β -catenin signaling in all neonatal fibroblasts, we produced crosses between $Pdgfra^+CreER^{T2}$ (Rivers et al., 2008) and *Ctnnb1* Exon3^{Flox/+} (Harada et al., 1999) mouse strains. Recombination of *Ctnnb1* Exon3^{Flox/+} (referred as $\Delta ex3$) produces a variant of β -catenin that is resistant to phosphorylation by glycogen synthase kinase 3 β and degradation by the adenomatous polyposis complex. Littermates were treated topically with 4-hydroxy-tamoxifen (4-OHT) on the day of birth and analyzed at different time points thereafter (Figure 3a).

By generating triple transgenics through crossing $Pdgfra^+CreER^{T2}$, *Rosa-CAG-LSL-tdTomato* (*tdTomato-LSL*), and *Ctnnb1* Exon3^{Flox/+} mice, we could show equal recombination efficiency whether or not β -catenin was stabilized. Fifty percent to 60% of all $Pdgfra^+$ fibroblasts were *tdTomato*⁺ at P4 in control and mutant ($\Delta ex3$) littermates (Figure 3b; see Supplementary Figure S1a online). *tdTomato*⁺ cells isolated from back skin at P4 did not express $\alpha 6$ integrin (a marker of epidermal keratinocytes), CD31 (endothelial cell marker), CD45 or other markers of hematopoietic lineages (see Supplementary Figure S1a, and data not shown).

The recombination efficiency was similar in different fibroblast subpopulations (Figure 3b). *Lrig1*⁺/*Sca1*⁻ cells are resident in the papillary dermis; *Dlk1*⁺/*Sca1*⁻ cells are a subpopulation of P2 reticular fibroblasts; *Sca1*⁺ cells, which can be *Dlk1*⁺ or *Dlk1*⁻, are found in the lower dermis and subdermal fat layer (Driskell et al., 2013). Analysis of skin sections confirmed that *tdTomato*⁺ cells were present in all dermal layers (Figure 3c and d).

A high abundance of nuclear β -catenin was detected in *tdTomato*⁺ fibroblasts of $\Delta ex3$ skin at P4 (see Supplementary Figure S1c–f) and was even more pronounced at P56 (Figure 3e–h). Furthermore, QPCR showed increased (albeit not significant) expression levels of known Wnt/ β -catenin target genes such as *Nov*, *Sp5*, and *Gpr165* (Hamburg-Shields et al., 2015) in flow-sorted *tdTomato*⁺ fibroblasts isolated from mutant skin compared with control skin (see Supplementary Figure S1g) at P4. Interestingly, at P56 expression levels of *Nov* were similar in *tdTomato*⁺/*Sca1*⁻ fibroblasts in wild-type and mutant dermis but significantly up-regulated in *tdTomato*⁺/*Sca1*⁺ fibroblasts, thereby reaching similar levels between papillary and reticular fibroblasts (see Supplementary Figure S1h).

No differences in skin morphology were observed between mutant and control mice at P4 (Figure 3i and j). However, at

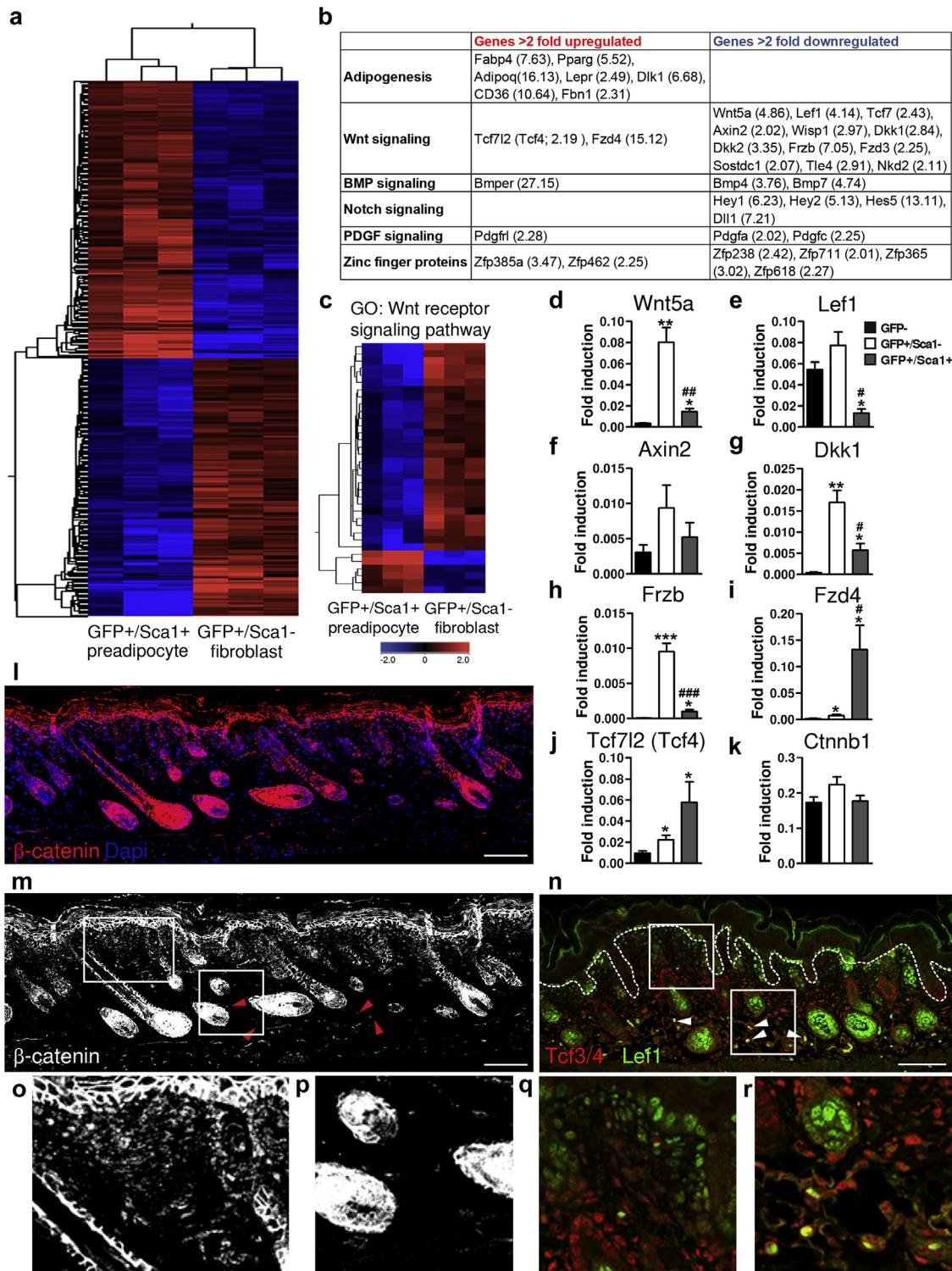


Figure 2. Distinct transcriptional signature of $Pdgfr\alpha EGFP^+/Sca1^+$ dermal cells. (a) Heat map showing hierarchical clustering (based on entities and samples) of all differentially regulated genes ($P < 0.05$, change >2 -fold) between $Pdgfr\alpha EGFP^+/Sca1^+$ and $Pdgfr\alpha EGFP^+/Sca1^-$ fibroblasts. (b) Selected genes up-regulated or down-regulated in $Sca1^+$ cells. Values in parentheses represent fold change of each gene. (c) Heat map showing hierarchical clustering (based on entities) of all regulated genes in the Gene Ontology term “Wnt receptor signaling pathway”. (d–k) Quantitative real-time PCR analysis of mRNA levels in sorted cell populations, normalized to *Gapdh* gene expression. Error bars represent standard error of the mean of replicates from four mice. * $P \leq 0.05$, ** $P \leq 0.005$, *** $P \leq 0.0005$ compared with GFP^- cells; * $P \leq 0.05$ compared with $GFP^+/Sca1^-$ cells. (l, m) Immunofluorescent staining of neonatal skin with an antibody detecting β -catenin. Red arrowheads show β -catenin $^+$ fibroblasts in the reticular dermis. 4', 6-diamidino-2-phenylindole labels nuclei. Scale bar = 200 μ m. (n) Section of P1 back skin immunostained for Tcf3/4 (red) and Lef1 (green). White arrowheads indicate double-labeled cells. Dashed lines demarcate epidermal-dermal boundary. Scale bar = 100 μ m. (o–r) Higher-magnification images of the boxed areas in (m, n), showing upper (o, q) and lower (p, r) dermis. BMP, bone morphogenic protein; DAPI, 4', 6-diamidino-2-phenylindole; GO, Gene Ontology; PDGF, platelet-derived growth factor.

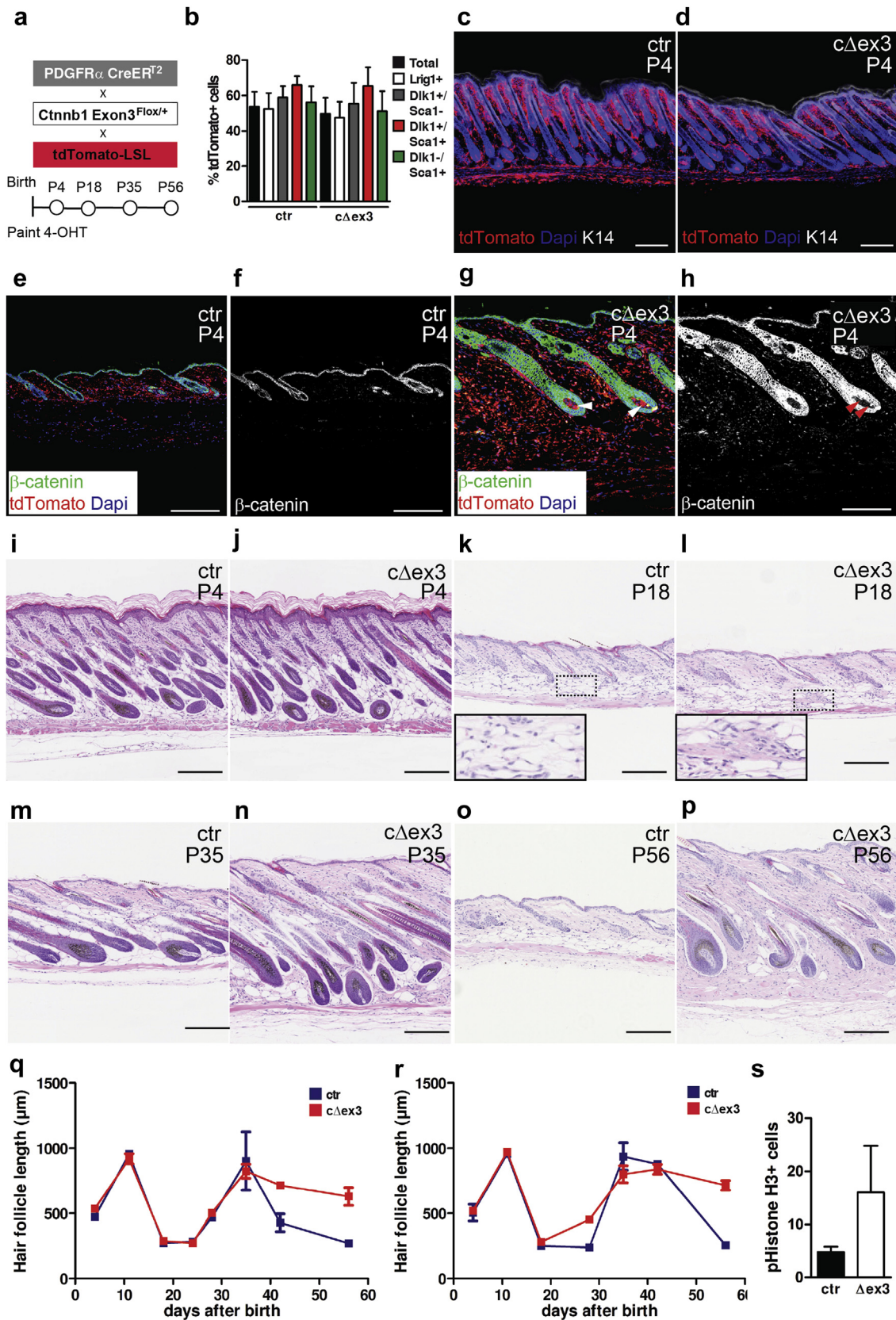


Figure 3. β -Catenin stabilization in dermal fibroblasts via *Pdgfr α CreER^{T2}*. (a) Schematic illustration of experimental strategy. (b) Recombination efficiency of *Pdgfr α CreER^{T2}*. Bar graph showing percentage of tdTomato⁺ cells within different fibroblast subsets after gating for ITGA6/LIN⁺/CD31⁻ cells 2 days after 4-OHT–mediated recombination. Data are reported as mean \pm standard error of the mean of triplicate samples in a representative experiment (n = 2–3 independent experiments). (c, d) tdTomato expression in 4-OHT–treated dorsal skin from (c) *Pdgfr α CreER^{T2}* \times tdTomato-LSL \times *Ctnnb1 Exon3^{+/+}* (control) and (d) *Pdgfr α CreER^{T2}* \times tdTomato-LSL \times *Ctnnb1 Exon3^{Flox/+}* (*cΔex3*) mice at P4. (e–h) Strong β -catenin staining is detected in tdTomato⁺ fibroblasts of mice

P18 we observed fibroblast-rich regions within the adipocyte layer of *c Δ ex3* mice (Figure 3k and l). At P35 these fibrotic regions were prominent (Figure 3m and n), and at P56 the adipocyte layer had been largely replaced by fibrotic dermis (Figure 3o and p).

To assess whether Wnt/ β -catenin signaling in fibroblasts affects the hair cycle, we classified different stages of HF's according to their morphology (Muller-Rover et al., 2001; Paus et al., 1999) and also examined their length. For each time point we examined at least 8 HF's per skin sample and skin biopsies from 2–8 different mice of the same genotype. We examined skin at P4 and P11 (n = 3–4), during the growth phase of HF morphogenesis; at P18 (n = 3–5), P24 (n = 2–4), and P28 (n = 2), during the first postnatal telogen; at P35 (n = 6), during anagen; and at P42 (n = 4–8) and P56 (n = 3–6), when the follicles are entering catagen and the second telogen, respectively. Regardless of genotype and age, all HF's were synchronized, with the exception of P35 *c Δ ex3* mice, when two of eight mice were still in telogen and the others were in anagen.

HF morphogenesis occurred normally in *c Δ ex3* mice (day 4 and 10; Figure 3q and r), as did the first telogen (day 18) and first anagen (day 35; Figure 3q and r). However, from day 42 the hair cycle was disturbed in both male (Figure 3q) and female (Figure 3r) *c Δ ex3* mice, and *c Δ ex3* follicles remained in anagen, as assessed both by morphology and length, when wild-type follicles were entering telogen (Figure 3o–r). Based on the observation that in two of eight mutant mice the HF's were still in telogen at P35, which were not scored in (Figure 3m and n), we speculate that there may be an extended growth phase before the second catagen. This is supported by the observation that there was an increased number of proliferating phosphohistone H3⁺ cells in the outer root sheath of HF's in mutant mice (Figure 3s). Nevertheless, the HF's in mutant skin eventually entered catagen, and all HF's were in telogen at the age of 3 months (n = 4; see Supplementary Figure S1i and j). Thus, our findings indicate that fibroblast-specific β -catenin stabilization perturbs the hair cycle and extends anagen.

Constitutive β -catenin activation results in dermal fibrosis

To characterize the effect of activated Wnt/ β -catenin signaling in fibroblasts, we focused on P35 skin (Figure 4). The fibrotic areas within the adipose layer of *c Δ ex3* dermis labeled pink with the histochemical Herovici's stain, indicative of the mature fibrillar collagen (Collins et al., 2011) (Figure 4a and b). QPCR showed reduced expression of differentiation markers such as *Fabp4*, *Perilipin*, and *Cebp α* (Figure 4c) in mutant *tdTomato⁺/Sca1⁺* fibroblasts compared with controls. Immunostaining confirmed reduced protein expression of *Perilipin* and *Fabp4* but showed higher levels of the preadipocyte marker *Cd24*

(Figure 4d–i). The reduction in the number of differentiated adipocytes was confirmed by LipidTox (Invitrogen/Thermo Fisher Scientific, Waltham, MA) staining (Figure 4j and k) and was statistically significant (Figure 4l). Fibroblast proliferative activity, measured by 5-Ethynyl-2'-deoxyuridine (EdU) labeling, was increased in both the adipocyte layer and in the rest of the dermis, including papillary fibroblasts of the dermal sheath and reticular fibroblasts, the effect being most pronounced in the adipocyte layer (Figure 4m–o). However, we did not detect significant numbers of EdU⁺ DP cells, consistent with our previous finding that the number of proliferating cells in adult DP is very low, even when β -catenin is stabilized and the DP increases in size (Kaushal et al., 2015).

Selective Wnt/ β -catenin stabilization in *Dlk1⁺* fibroblasts results in fibrosis within the adipose layer

Given the differential expression of adipogenic genes in *Sca1⁺* and *Sca1⁻* fibroblasts at P2 (Figure 2) and the fibrosis within the adipose layer on fibroblast-specific stabilization of β -catenin (Figure 3), we hypothesized that the fibrotic effect of activating Wnt/ β -catenin signaling in all *Pdgfra⁺* fibroblasts would be reproduced by selectively targeting the lower dermal lineage during skin development. Because fibroblasts that express *Dlk1* at E16.5 give rise to the *Sca1⁺* fibroblasts and mature adipocytes present at P2 and in adult skin (Driskell et al., 2013), we crossed *Ctnnb1 Exon3^{Flox/+}*, *Dlk1CreER^{T2}*, and *tdTomato-LSL* mice and treated them with tamoxifen at E16.5 to target the lower dermal lineage (Figure 5a).

When fibroblasts were isolated at E18.5, 2 days after tamoxifen injection in utero, 3% of total *Pdgfra⁺* fibroblasts were labeled (Figure 5b; Figure S1b). Ten percent to 15% of *Dlk1⁺/Sca1⁻* and *Dlk1⁺/Sca1⁺* cells were labeled, compared with 2% of *Dlk1⁻/Sca1⁺* cells (Figure 5b; see Supplementary Figure S1b) and 1% of *Lrig1⁺* papillary fibroblasts, confirming the selectivity of targeting. *tdTomato⁺* fibroblasts comprised 30% *Dlk1⁺/Sca1⁻*, 55% *Dlk1⁺/Sca1⁺* cells, and 10% *Dlk1⁻/Sca1⁺* cells (Figure 5c). It is most likely that *tdTomato⁺* cells within the *Dlk1⁻/Sca1⁺* fibroblast population correspond to cells that were *Dlk1⁺* at E16.5 but subsequently down-regulated *Dlk1* expression (Driskell et al., 2013). When examined at P56, *tdTomato⁺* cells were confined to the lower dermis in both control and *Dlk1LTD Δ ex3* skin (Figure 5d and e). In control skin most *tdTomato⁺* cells had the morphology of mature adipocytes, whereas in *Dlk1LTD Δ ex3* skin the *tdTomato⁺* cells had a fibroblastic morphology (Figure 5d and e; mature adipocytes are labeled with asterisks in Figure 5d).

In contrast to the effect of activating Wnt/ β -catenin signaling in all fibroblasts, selective activation in *Dlk1⁺* cells did not disturb the hair cycle, and at P56 both control and *Dlk1LTD Δ ex3* skin was in telogen (Figure 5f and g). Nevertheless, there was an accumulation of fibroblasts within the adipose layer in

with activated Wnt/ β -catenin signaling. Note that the *PDGFR α CreER^{T2}* transgene is also active in cells of the dermal papilla (white arrowheads in g). Red arrowheads in (h) depict β -catenin⁺ cells in the dermal papilla. (i–p) Paraffin sections of back skin of control and mutant (*c Δ ex3*) littermates stained for hematoxylin and eosin at (i, j) P4, (k, l) first telogen (P18), (m, n) anagen (P35), and (o, p) second telogen (P56). Boxed areas in (k, l) are shown as higher-magnification inserts. Scale bars = 200 μ m. (q, r) Hair follicle length measured in (q) male and (r) female *c Δ ex3* and control mice at P4, P11, P18, P24, P28, P35, P42, and P56 (n = 2–8). Data points are reported as mean \pm standard error of the mean. (s) Quantification of proliferating, phosphohistone H3⁺ cells in the outer root sheath of hair follicles in immunostained skin sections (n = 3 biological samples; \geq 5 hair follicles per biological sample were scored). 4-OHT, 4-hydroxy-tamoxifen; ctr, control; Dapi, 4', 6-diamidino-2-phenylindole; K14, keratin 14.

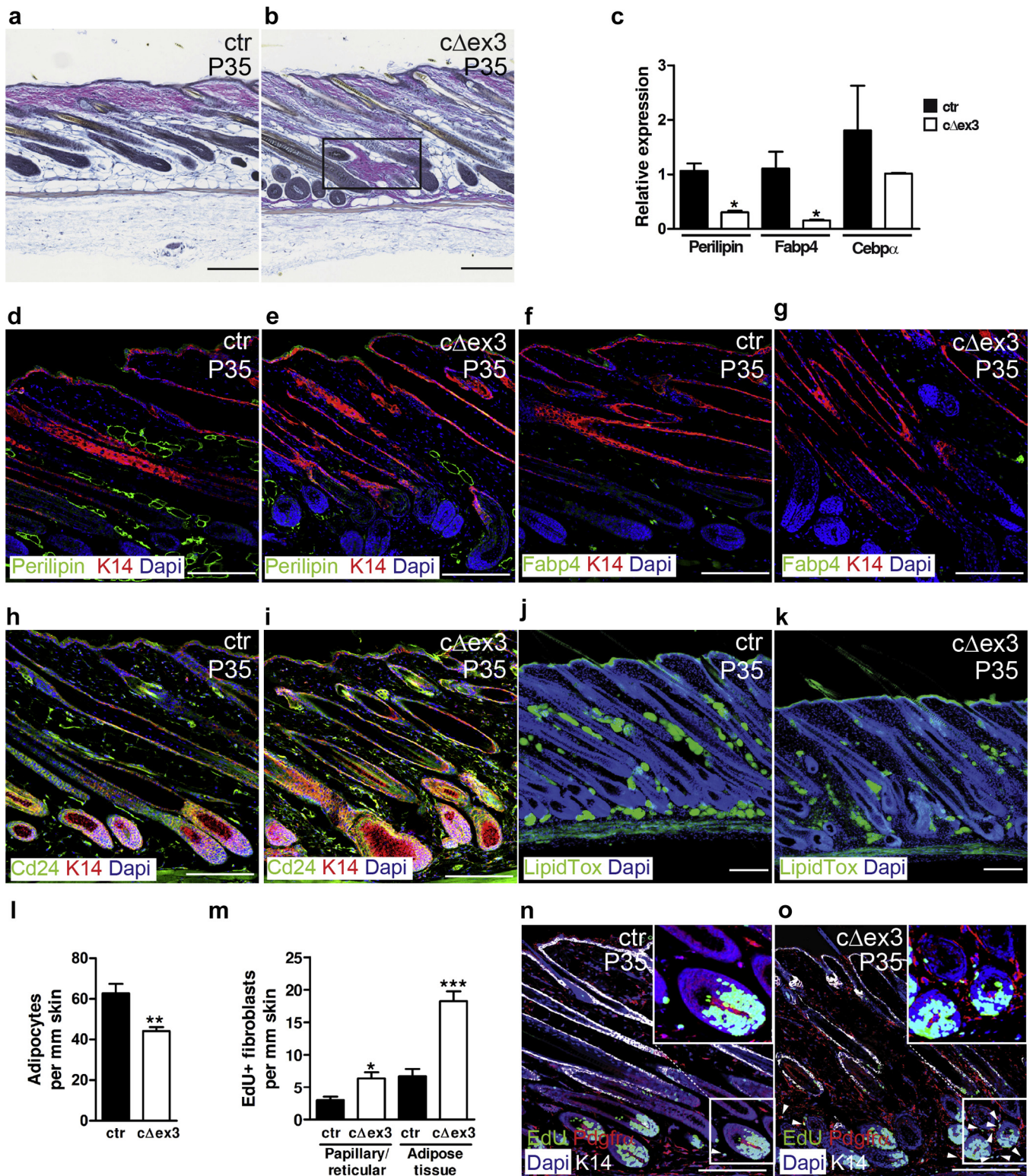


Figure 4. Induction of dermal fibrosis and proliferation by β -catenin stabilization. (a, b) Herovici's staining differentiates between immature collagen fibers (blue) versus mature collagen (pink). Note fibrotic region with mature extracellular matrix in (b) (boxed). (c) Relative expression of adipocyte differentiation genes in flow-sorted tdTomato⁺ fibroblasts. Data represent mean \pm standard error of the mean (n = 3). * $P \leq 0.05$. (d–i) Immunostained paraffin sections of 35-day-old mutant and control skin. (j, k) Whole-mount thick sections stained with LipidTox (green) with DAPI counterstain (blue). (l, m) Quantification in paraffin sections of P35 skin of (l) adipocytes and (m) EdU⁺ fibroblasts in the adipocyte layer and interfollicular dermis (including papillary fibroblasts, dermal sheath, and reticular fibroblasts). The boundary between papillary/reticular and adipocyte layers was defined by the interface between the bottom of the reticular layer and the upper layer of differentiated adipocytes. Data points represent mean \pm standard error of the mean; n ≥ 5 for each group. * $P \leq 0.05$; ** $P \leq 0.005$; *** $P \leq 0.0005$. (n, o) Skin labeled with EdU (green) for 4 hours before harvesting, costained for Pdgfra (red), keratin 14 (white), and DAPI (blue). White arrowheads indicate EdU⁺ fibroblasts within the adipose layer. Inserts are higher-magnification images of the boxed areas. Scale bars = 200 μ m. ctr, control; DAPI, 4', 6-diamidino-2-phenylindole; K14, keratin 14.

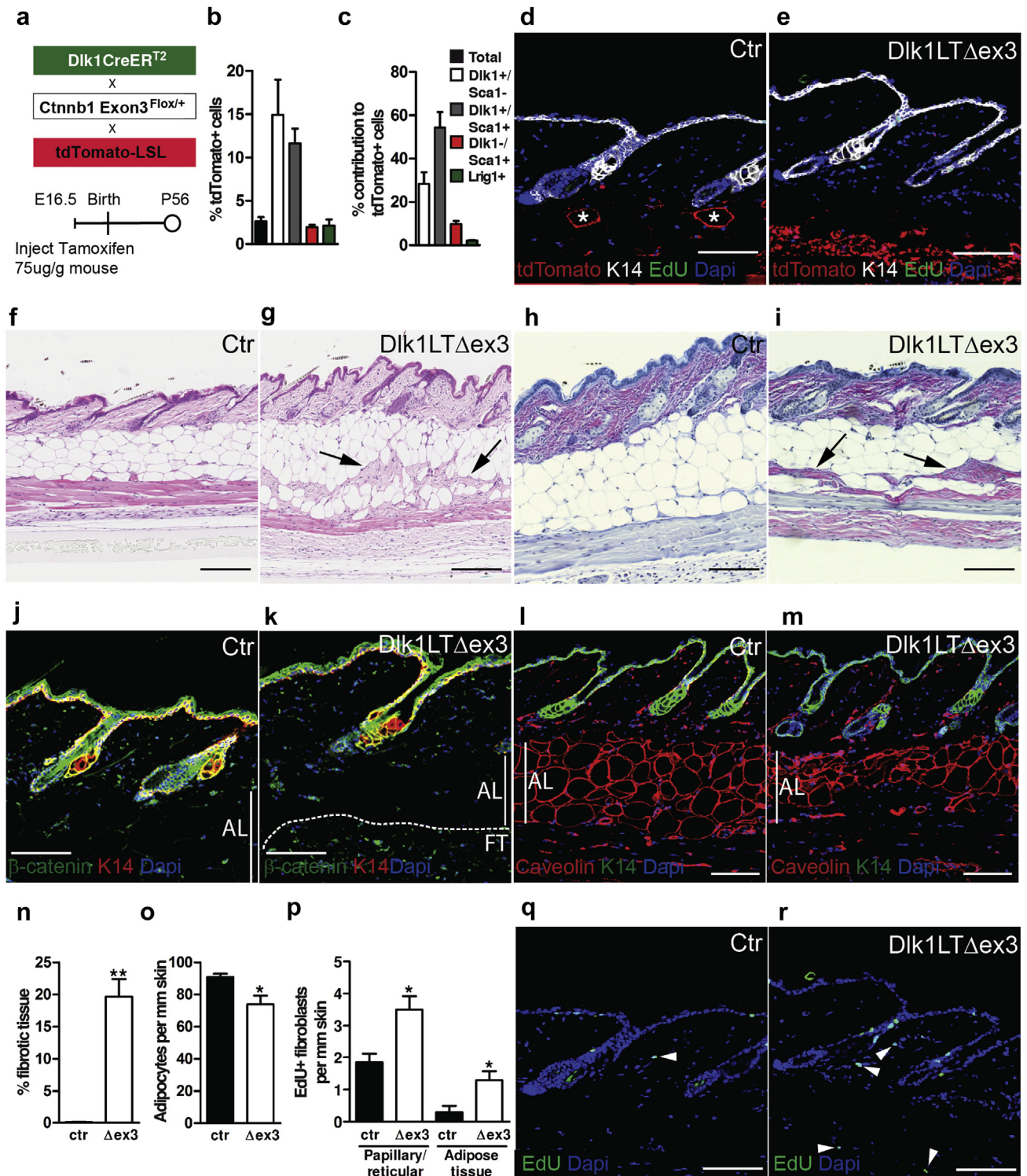


Figure 5. β -Catenin stabilization in the lower dermis via *Dlk1CreERT2*. (a) Schematic illustration of experimental strategy. (b, c) Quantification of tdTomato⁺ cells in E18.5 dermal cell suspensions (ITGA6⁻/LIN⁻/CD31⁻) 2 days after 4-OHT injection. (b) Percentage of tdTomato⁺ cells in each fibroblast subpopulation. (c) Contribution of each fibroblast subpopulation to tdTomato⁺ fibroblasts. Data are presented as mean \pm standard error of the mean of quadruplicate samples in a representative experiment (n = 3 independent experiments). (d, e) tdTomato-expressing cells in P56 back skin of *Dlk1CreERT2* \times tdTomato-LSL \times *Ctnnb1 Exon3^{Flox/+}* (control) and *Dlk1CreERT2* \times tdTomato-LSL \times *Ctnnb1 Exon3^{Flox/+}* (*Dlk1LT Δ ex3*) mice. Asterisks in (d) indicate terminally differentiated adipocytes. (f, g) Hematoxylin and eosin and (h, i) Herovici's staining of paraffin sections of P56 control and *Dlk1LT Δ ex3* mouse back skin. Arrows in (g) and (i) indicate fibrotic regions. (j–m) P56 control and *Dlk1LT Δ ex3* back skin labeled for β -catenin or caveolin-1 and keratin 14, counterstained with DAPI. Vertical lines indicate thickness of adipocyte layer. Dashed line in (k) demarcates fibrotic tissue (FT). (n, o) Quantification of fibrotic area shown as percentage of the adipocyte layer (n) and number of adipocytes (o). (p) Quantification of EdU-labeled fibroblasts in the interfollicular dermis (including papillary fibroblasts, dermal sheath, and reticular fibroblasts) and adipose layer (defined as in Figure 4m) after a 2-hour EdU pulse. Data are presented as mean \pm standard error of the mean of triplicate samples in a representative experiment (n = 3–5). **P* \leq 0.05; ***P* \leq 0.005. (q, r) EdU staining of sections shown in (d) and (e). Scale bars = 200 μ m. 4-OHT, 4-hydroxy-tamoxifen; AL, adipocyte layer; ctr, control; DAPI, 4', 6-diamidino-2-phenylindole; K14, keratin 14.

Dlk1LT Δ ex3 skin (Figure 5f and g). These regions stained positively for fibrillar ECM using Herovici's dye (Figure 5h and i) and expressed high levels of β -catenin (Figure 5j and k). The reduction in adipocyte numbers was confirmed by labeling for caveolin-1, a marker for preadipocytes and adipocytes (Figure 5l and m) and was statistically significant, in accordance with the appearance of fibrotic lesions (Figure 4n and o). Stabilization of β -catenin via Dlk1CreER^{T2} also resulted in an increase in fibroblast proliferation both in the adipocyte layer and throughout the dermis (Fig. 5p–r).

Postnatal Wnt/ β -catenin stabilization inhibits adipogenesis of Sca1⁺ fibroblasts in culture

To establish whether β -catenin stabilization within preadipocytes resulted in an inhibition of differentiation, we analyzed the behavior of single cells captured in ECM-functionalized hydrogels, as described previously (Driskell et al., 2012; Driskell et al., 2013). Pdgfr α CreER^{T2}, tdTomato-LSL, and Ctnnb1 Exon3^{Flox/+} mice were crossed and treated with 4-OHT on the day of birth (Figure 6a). Sca1⁺ tdTomato⁺ fibroblasts were isolated by flow cytometry 2 days later (Figure 6b and c). Activation of Wnt/ β -catenin signaling did not affect the proportion of Sca1⁺ cells that expressed the preadipocyte marker Cd24 (Festa et al., 2011) (Figure 6d).

Sca1⁺ cells were encapsulated at clonal density in 3-dimensional hydrogels and cultured in control or adipogenic medium. After 10 days in culture, individual clones were scored for cell number and the total intensity of LipidTox staining (Figure 6e). Whereas β -catenin stabilization in vivo stimulated proliferation within the adipose layer (Figure 4m), there was no effect on clone size when Sca1⁺ cells were cultured in adipogenic medium, and in standard medium the only effect was to increase the percentage of two cell clones at the expense of clones with higher cell numbers (Figure 6f and g). Wnt/ β -catenin signaling activation did, however, decrease adipocyte differentiation, as evaluated by decreased LipidTox staining, both in standard medium (Figure 6h) and in medium supplemented with adipogenic factors, regardless of clone size (Figure 6i). These findings suggest that the effect of β -catenin stabilization in neonatal fibroblasts is to prevent Sca1⁺ fibroblasts from undergoing adipocyte differentiation in a cell-autonomous manner, rather than changing the proportion of Cd24⁺/Sca1⁺ preadipocytes.

DISCUSSION

Here we have examined the effect of dermal Wnt/ β -catenin signaling in the context of fibroblast heterogeneity. We show that expression of Wnt pathway genes such as *Wnt5a*, *Lef1*, *Tcf4*, or *Dkk1* differs between upper (Sca1⁻) and lower (Sca1⁺) dermis. Interestingly, immunostaining showed that β -catenin and *Lef1* are more abundant in Sca1⁻ cells. β -Catenin stabilization in all fibroblast populations in neonatal skin resulted in a decrease in mature adipocytes and the appearance of fibrotic regions in the adipose layer, accompanied by stimulation of fibroblast proliferation throughout the dermis. The replacement of adipocytes by ectopic reticular fibroblasts also occurred when the lower dermal lineage was selectively targeted at E16.5, before adipocyte differentiation.

Our in vitro studies showed that β -catenin stabilization did not drive fibroblast proliferation cell-autonomously. The effect of β -catenin stabilization was to inhibit terminal differentiation of Sca1⁺ cells rather than to promote expansion of preadipocytes or selective proliferation of reticular fibroblasts. This is similar to the effect of β -catenin stabilization on cultured human keratinocytes, which is to expand the stem cell compartment without stimulating proliferation (Zhu and Watt, 1999). However, although we did not detect an expansion of preadipocytes within 4 days of β -catenin stabilization in vivo, Cd24 expression was increased in P35 skin. This could either be caused by an expansion of preadipocytes at a later stage, which is supported by increased fibroblast proliferation in vivo, or by the differentiation defect.

Our conclusion that targeting the lower dermal lineage accounts for the appearance of fibrotic regions is consistent with other studies highlighting the contributions of different dermal cell subpopulations to fibrosis. For example, fibroblasts that express engrailed 1 during development are responsible for the bulk of ECM deposition in dorsal dermis and mediate dermal fibrosis in response to irradiation (Rinkevich et al., 2015). Other dermal subpopulations that contribute to fibrosis include Sox2⁺ cells (Liu et al., 2014) and adiponectin-positive adipocyte precursors (Marangoni et al., 2015). In addition, Adam12⁺ perivascular mesenchymal cells expressing Pdgfr α and Sca1 are profibrotic in response to injury (Dulauroy et al., 2012).

The inhibition of adipocyte differentiation was not the only effect of dermal β -catenin activation that we observed. There was an increase in proliferation throughout the dermis, consistent with an earlier report (Cheon et al., 2002), and a disruption of the HF cycle. The effects on the hair cycle cannot be attributed solely to a decrease in mature adipocytes (Donati et al., 2014; Festa et al., 2011), because they were observed when we targeted all fibroblast subpopulations via Pdgfr α CreER^{T2} and not when we selectively targeted the lower dermal lineage. This raises an interesting question as to whether increased proliferation of the fibroblast subpopulations that are known to regulate hair growth, in particular the DP, dermal sheath, and other papillary fibroblasts (Driskell et al., 2013; Enshell-Seijffers et al., 2010; Kaushal et al., 2015), is responsible. We have previously shown that β -catenin stabilization in Prominin-1-expressing DP cells results in an increase in DP size, but because the number of EdU⁺ cells is very low, the increase could be attributable to a number of factors, such as increased migration from the dermal sheath (Kaushal et al., 2015). Because the Pdgfr α CreER^{T2} transgene is active in DP cells (Figure 3g and h), it is possible that the perturbed hair cycle reflects, at least in part, Wnt/ β -catenin activation in DP cells. The effect of β -catenin stabilization on proliferation in the upper and lower dermis could either be direct or indirect. An indirect effect could be via dermal ECM, because Tcf-mediated transcription of several ECM protein-coding genes has recently been shown in a fibrosis model of sustained β -catenin activity in Hoxb2-derived ventral fibroblasts (Hamburg-Shields et al., 2015).

Our findings are in good agreement with previous reports that β -catenin plays a role in skin fibrosis (Beyer et al., 2012)

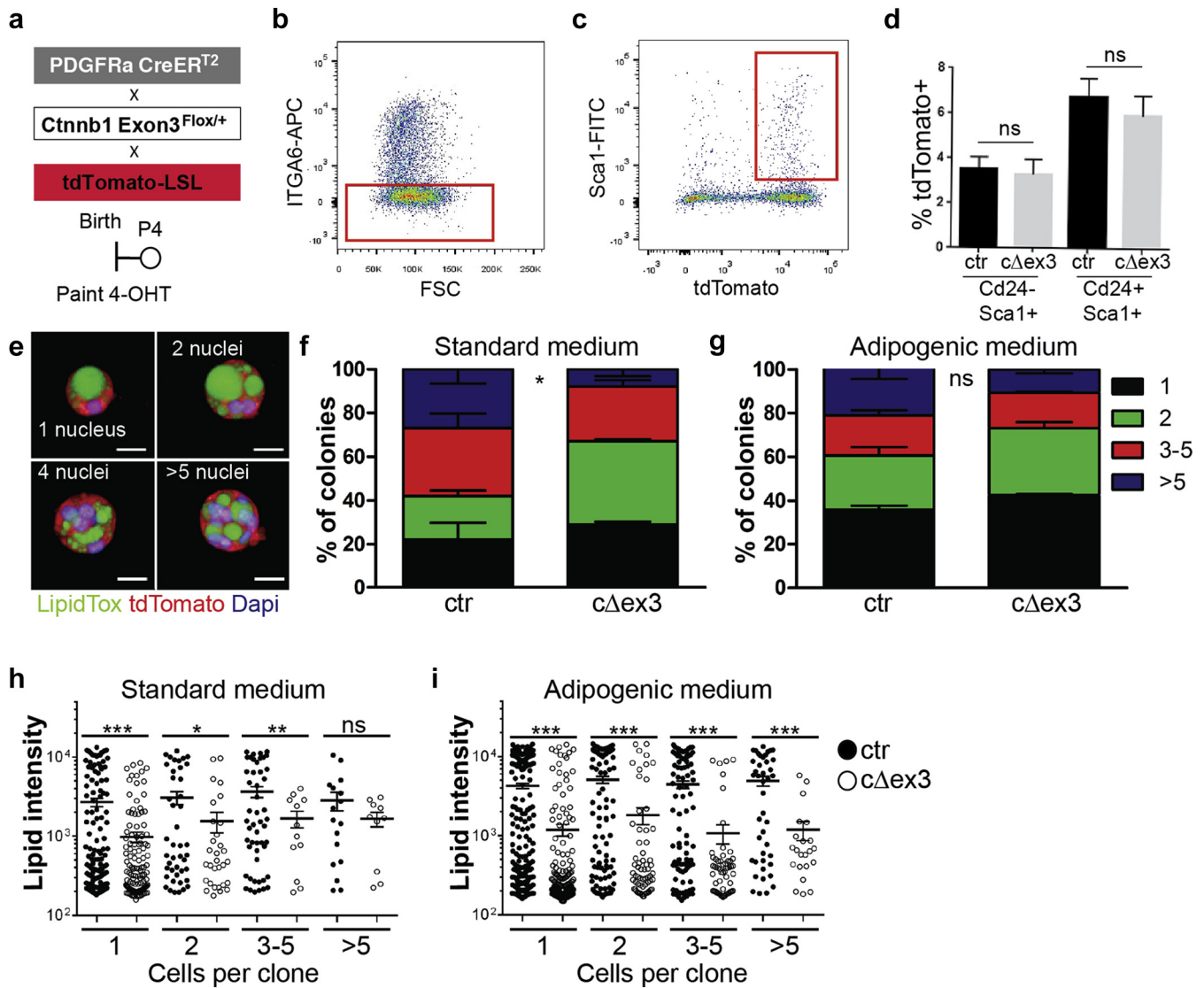


Figure 6. Effect of β -catenin stabilization on adipocyte differentiation in cultured Sca1⁺ fibroblasts. (a) Schematic illustration of experimental strategy. (b–d) Sca1⁺/tdTomato⁺ targeted fibroblasts from dermal cell suspensions of PDGFR α CreER^{T2} × tdTomato-LSL × Ctnnb1 Exon3^{+/+} (control) and PDGFR α CreER^{T2} × tdTomato-LSL × Ctnnb1 Exon3^{Flox/+} (c Δ ex3) littermates were isolated by flow cytometry. (b, c) Gating out α 6 integrin-positive cells (ITGA6; keratinocytes) (b) and positive selection for Sca1⁺/tdTomato⁺ cells (c). (d) Recombination efficiency (percentage tdTomato⁺ cells) in Cd24⁺/Sca1⁺ and Cd24⁻/Sca1⁺ cells. Data are presented as mean \pm standard error of the mean of triplicate samples in a representative experiment (n = 3 independent experiments). (e) Examples of individual colonies formed by Sca1⁺ fibroblasts stained for LipidTox (green), tdTomato (red), and DAPI (blue). Scale bars = 10 μ m. (f, g) Percentage of colonies containing 1, 2, 3–5, or more than 5 cells in standard (f) and adipogenic (g) medium. (h, i) Total LipidTox fluorescence (lipid intensity) per clone in control and mutant (c Δ ex3) cultures grown in standard (h) or adipogenic (i) medium. (f–i) n = 2–3 biological replicates and 2 technical replicates. *P \leq 0.05, **P \leq 0.01, ***P \leq 0.005. (f, g) two-way analysis of variance with a Bonferroni posttest. (h, i) 25% confidence intervals are shown. 4-OHT, 4-hydroxy-tamoxifen; ctr, control DAPI, 4', 6-diamidino-2-phenylindole; FSC, forward scatter; ns, difference not significant.

and causes a down-regulation of adipogenic effector pathways, such as cEBP/PPAR γ , in culture (Gesta et al., 2007). In addition, expression of the Wnt inhibitor Dkk1 interferes with profibrotic signaling (Akhmetshina et al., 2012). Together, these studies suggest that pharmacological modulation of Wnt signaling could be beneficial in the treatment of fibrotic skin diseases, including scleroderma (Ohgo et al., 2013). Similar mechanisms could also be responsible for the regulation of mesenchymal progenitors in other organs, including Pdgfr α ⁺/Sca1⁺ muscle fibroblasts with proliferative and myofibroblast/adipogenic potential in response to muscle regeneration and ectopic fat formation (Uezumi et al., 2010).

MATERIALS AND METHODS

In vivo experiments

The following mouse strains were maintained on a C57 Bl6/CBA background: Dlk1CreER^{T2} Institut Clinique de la Souris (ICS, Illkirch-Graffenstaden Cedex Alsace, France), Pdgfr α EGFP (Pdgfr α H2B-eGFP) (Jackson Laboratories, Bar Harbor, ME), Ctnnb1lox(ex3)^{+/+} (Harada et al., 1999), Pdgfr α CreER^{T2} (Rivers et al., 2008) and Rosa-CAG-LSL-tdTomato (Jackson Laboratories; 007905) strains were maintained as homozygotes. Cre-mediated recombination was induced by topical application of 2 mg of 4-hydroxy-tamoxifen (Sigma, St. Louis, MO; diluted in acetone + 10% DMSO) on the back skin of neonatal pups at P0–P1. For lineage tracing experiments, plugged females received a single intraperitoneal injection of

25 μg of tamoxifen per gram of body weight at E16.5. Tamoxifen was dissolved in corn oil (10–20 mg/ml) by intermittent sonication at 37°C for 20–30 minutes. Pups were harvested and fostered after surgical removal between E18.5 and E21. For in vivo proliferation assays, mice received a dose of 500 μg 5-ethynyl-2'-deoxyuridine (EdU; 2.5mg/ml in phosphate buffered saline) by intraperitoneal injection 2–4 hours before they were killed. Cohorts included male and/or female littermates, and results are representative of at least three biological samples. All experimental procedures were carried out under the terms of a UK Home Office project license after ethical review at Cambridge University or King's College London.

Histology

Skin samples were harvested and processed to generate paraffin (5 μm) or thick cryopreserved whole-mount tissue (50–100 μm) sections as previously described (Collins et al., 2011; Driskell et al., 2013). Immunostaining was performed using the following antibody combinations: rabbit anti-Rfp (1:300; Rockland, Limerick, PA)/rabbit anti-Perilipin 1A (1:100; Abcam, Cambridge, UK)/rabbit anti-Caveolin-1 (1:100; Abcam); rabbit anti-Fabp4 (1:100; Abcam); donkey anti-rabbit Alexa Fluor 555, 594, or 488; goat anti-PDGFRα and goat anti-Sca1 (1:100; R&D Systems, Minneapolis, MN); donkey anti-goat Alexa Fluor 488 or 647; chicken or rabbit anti-Keratin 14 (1:100; Covance, Princeton, NJ); goat anti-chicken Alexa Fluor 647 or 555; mouse β-catenin (1:100; BD Transduction, Lexington, KY); donkey anti-mouse Alexa Fluor 594 or 488; rabbit anti-TCF3/4 (1:100; Abcam) and anti-Lef1 (1:100; Cell Signalling, Danvers, MA); Alexa Fluor 488 conjugated anti-CD24 (1:300; BD Pharmingen, Franklin Lakes, NJ). LipidTox (1:500 in phosphate buffered saline; Invitrogen/Thermo Fisher Scientific, Waltham, MA) was used to stain neutral lipids in adipocytes. ProLong Gold antifade reagent (Invitrogen) or glycerol was used for mounting slides or whole-mount sections, counterstained with 4', 6-diamidino-2-phenylindole (DAPI). The EdU click-it imaging kit (Invitrogen) was used for detecting incorporated EdU nucleoside analogs in proliferating cells. Herovici's staining was performed as previously described (Collins et al., 2011).

Image acquisition and quantification

Immunostained tissue sections were imaged using a Nikon A1R confocal microscope. Adobe Photoshop CS6 (Adobe, San Jose, CA) was used to adjust images and correct background. Bright field images were collected using either a Hamamatsu NanoZoomer slide scanner (Hamamatsu, Japan) or a Zeiss Axiophot microscope (Carl Zeiss, Oberkochen, Germany) with a ×10 objective and an Axio-Cam HRc camera. Image measurements were performed on at least six microscopic fields per biological sample.

Cell isolation and flow cytometry

Dermis was separated from back skin of embryos (E18.5–E19.5) or postnatal pups (P2–P4) by incubation with thermolysin (0.25 mg/ml) (Sigma T7902) overnight at 4°C, digested in Dulbecco's Modified Eagle's Medium + 10% fetal bovine serum containing 2.5 mg/mL collagenase I (Gibco 17100-017; Gibco/Thermo Fisher Scientific, Waltham, MA), and further processed as previously described (Collins et al., 2011). Cells were labeled in phosphate buffered saline + 10% fetal bovine serum TruStain fcX anti-mouse blocking buffer with the following antibodies: anti-mouse Ly-6A/E (Sca-1)-Alexa Fluor 488, 700, or BV605 (clone D7; 1:200); CD140a/Pdgfra-APC (clone APA5; 1:20); CD45-Alexa Fluor 700

(clone 30-F11; 1:100); CD24-Fitc (Clone M1/69; 1:100) (eBioscience, San Diego, CA); Lrig1-Alexa Fluor 488 (polyclonal; 1:20) (RnD Systems); anti-rat Dlk1-Fitc (clone 24-11; 1:20) (MBL International, Woburn, MA); anti-mouse-CD31-Alexa Fluor 647 (BD Pharmingen); APC Mouse Lineage Antibody Cocktail (BD Pharmingen); and anti-human CD49f-Alexa Fluor 647 (clone NK1-GoH3; 1:20) (AbD Serotec, Kidlington, UK). A BD LSRFortess a (Becton Dickinson, Franklin Lakes, NJ) was used for flow cytometry and an Aria II (Becton Dickinson, Franklin Lakes, NJ) for sorting fibroblasts. Dead cells were excluded from analysis using DAPI. Fibroblasts were either sorted for CD140α expression or negatively selected by excluding epidermal, endothelial, and immune cells from the cell suspension (ITGA6/LIN/CD31). Data analysis and visualization were performed using FlowJo software version 7.6.5 (Tree Star, Ashland, OR).

Hydrogel culture and high-content imaging

Sorted fibroblasts were collected and encapsulated in Extracel (Glycosan Biosystems) as previously described (Driskell et al., 2012), at a density of 5×10^5 /ml in μClear 96-well plates (Corning). Cultures were maintained for 10 days at 37°C/5% CO₂ in standard medium (Dulbecco's modified Eagle's medium + 10% fetal bovine serum + 1% penicillin/streptomycin) or Adipogenic medium (StemXVivo Osteogenic/Adipogenic Base Media with Adipogenic Supplement; R&D Systems), and the medium was changed every 2–3 days.

Cultures were fixed with 4% paraformaldehyde for 10 minutes, washed twice in phosphate buffered saline, permeabilized with 0.1% Triton X-100 for 5 minutes and stained with LipidTox, DAPI, and rabbit anti-Rfp (1:300 dilution; Abcam). Multiple image stacks of each colony were recorded using an Operetta High Content Imaging system (Perkin Elmer, Waltham, MA). Spheres were identified by staining for tdTomato, and the number of nuclei per sphere was determined using quantification algorithms in the Columbus analysis software (Perkin Elmer, Waltham, MA). The fluorescence intensity of LipidTox staining was measured for each sphere.

Quantification and Statistics

GraphPad Prism 6 software (GraphPad Software Inc., La Jolla, CA) was used for all analyses of numerical data and generation of graphs and statistical tests, including one-way analysis of variance or Student *t* test. Error bars represent standard error of the mean.

Microarray

Genome-wide expression profiling was carried out by the Paterson Institute Microarray Core Facility, as described previously (Collins et al., 2011). The data are deposited in the National Institutes of Health GEO repository under accession number GSE76751. Complementary DNA was hybridized to Affymetrix MG430.2A arrays (Affymetrix, Santa Clara, CA). Array images produced by the Affymetrix PICR 3000 scanner were imported as CEL files into Genespring GX11 (Agilent Technologies, Santa Clara, CA) for analysis. Robust Multi-array Average normalization (baseline to median of all samples) was used. Analyses were performed on genes selected for expression above the bottom 20th percentile in all three samples within at least one of two experimental groups. To identify differentially expressed genes, we compared the two groups using the Student *t* test (*P*-value cut-off of 0.05). Entities regulated by greater than 2-fold were selected for further analysis.

ORCIDs

Beate M. Lichtenberger: <http://orcid.org/0000-0001-6882-0257>
Maria M. Mastrogiannaki: <http://orcid.org/0000-0003-4978-2237>
Fiona M. Watt: <http://orcid.org/0000-0001-9151-5154>

CONFLICT OF INTEREST

The authors state no conflict of interest.

ACKNOWLEDGMENTS

This work was supported by grants to FMW from the Medical Research Council and the Wellcome Trust. MM and BML were supported by long-term postdoctoral fellowships from the European Molecular Biology Organization (EMBO) and Federation of European Biochemical Societies (FEBS). We gratefully acknowledge excellent support from staff at King's College London and Wellcome Trust Centre for Stem Cell Research, particularly J. Harris, Head of the Nikon Microscopy Centre at King's. We gratefully acknowledge financial support in the form of access to the Biomedical Research Centre flow cytometry core of Guy's & St. Thomas' National Health Service (NHS) Foundation Trust.

AUTHOR CONTRIBUTIONS

MM and BML equally contributed to performing and analyzing the experiments shown in Figures 2–6. AR performed and analyzed the experiments shown in Figure 6. CAC generated and analyzed the microarray data, which were validated by RRD, and generated data in Figures 1 and 2. FMW contributed to experimental design and analysis. MM, BML, and FMW wrote the manuscript. All authors contributed to interpreting the findings and editing the final manuscript.

SUPPLEMENTARY MATERIAL

Supplementary material is linked to the online version of the paper at www.jidonline.org, and at <http://dx.doi.org/10.1016/j.jid.2016.01.036>.

REFERENCES

- Akhmetshina A, Palumbo K, Dees C, Bergmann C, Venalis P, Zerr P, et al. Activation of canonical Wnt signalling is required for TGF-beta-mediated fibrosis. *Nat Commun* 2012;3:735.
- Atit R, Sgaier SK, Mohamed OA, Taketo MM, Dufort D, Joyner AL, et al. Beta-catenin activation is necessary and sufficient to specify the dorsal dermal fate in the mouse. *Dev Biol* 2006;296:164–76.
- Beyer C, Schramm A, Akhmetshina A, Dees C, Kireva T, Gelse K, et al. Beta-catenin is a central mediator of pro-fibrotic Wnt signaling in systemic sclerosis. *Ann Rheum Dis* 2012;1:761–7.
- Cauchi S, Meyre D, Choquet H, Dina C, Born C, Marre M, et al. TCF7L2 variation predicts hyperglycemia incidence in a French general population: the data from an epidemiological study on the Insulin Resistance Syndrome (DESIR) study. *Diabetes* 2006;55:3189–92.
- Cheon SS, Cheah AY, Turley S, Nadesan P, Poon R, Clevers H, et al. Beta-catenin stabilization dysregulates mesenchymal cell proliferation, motility, and invasiveness and causes aggressive fibromatosis and hyperplastic cutaneous wounds. *Proc Natl Acad Sci USA* 2002;99:6973–8.
- Collins CA, Kretzschmar K, Watt FM. Reprogramming adult dermis to a neonatal state through epidermal activation of beta-catenin. *Development* 2011;138:5189–99.
- Donati G, Proserpio V, Lichtenberger BM, Natsuga K, Sinclair R, Fujiwara H, et al. Epidermal Wnt/beta-catenin signaling regulates adipocyte differentiation via secretion of adipogenic factors. *Proc Natl Acad Sci USA* 2014;111:E1501–9.
- Driskell RR, Giangreco A, Jensen KB, Mulder KW, Watt FM. Sox2-positive dermal papilla cells specify hair follicle type in mammalian epidermis. *Development* 2009;136:2815–23.
- Driskell RR, Juneja VR, Connelly JT, Kretzschmar K, Tan DW, Watt FM. Clonal growth of dermal papilla cells in hydrogels reveals intrinsic differences between Sox2-positive and -negative cells in vitro and in vivo. *J Invest Dermatol* 2012;132:1084–93.
- Driskell RR, Lichtenberger BM, Hoste E, Kretzschmar K, Simons BD, Charalambous M, et al. Distinct fibroblast lineages determine dermal architecture in skin development and repair. *Nature* 2013;504:277–81.
- Driskell RR, Watt FM. Understanding fibroblast heterogeneity in the skin. *Trends Cell Biol* 2015;25:92–9.
- Dulauroy S, Di Carlo SE, Langa F, Eberl G, Peduto L. Lineage tracing and genetic ablation of ADAM12(+) perivascular cells identify a major source of profibrotic cells during acute tissue injury. *Nat Med* 2012;8:1262–70.
- Enshell-Seiffers D, Lindon C, Kashiwagi M, Morgan BA. Beta-catenin activity in the dermal papilla regulates morphogenesis and regeneration of hair. *Dev Cell* 2012;18:633–42.
- Festa E, Fretz J, Berry R, Schmidt B, Rodeheffer M, Horowitz M, et al. Adipocyte lineage cells contribute to the skin stem cell niche to drive hair cycling. *Cell* 2011;146:761–71.
- Fujiwara H, Ferreira M, Donati G, Marciano DK, Linton JM, Sato Y, et al. The basement membrane of hair follicle stem cells is a muscle cell niche. *Cell* 2011;144:577–89.
- Gesta S, Tseng YH, Kahn CR. Developmental origin of fat: tracking obesity to its source. *Cell* 2007;131:242–56.
- Gupta RK, Arany Z, Seale P, Mepani RJ, Ye L, Conroe HM, et al. Transcriptional control of preadipocyte determination by Zfp423. *Nature* 2012;464:619–23.
- Hamburg-Shields E, DiNucio GJ, Mullin NK, Lafayatis R, Atit RP. Sustained beta-catenin activity in dermal fibroblasts promotes fibrosis by up-regulating expression of extracellular matrix protein-coding genes. *J Pathol* 2015;235:686–97.
- Hamilton TG, Klinghoffer RA, Corrin PD, Soriano P. Evolutionary divergence of platelet-derived growth factor alpha receptor signaling mechanisms. *Mol Cell Biol* 2003;23:4013–25.
- Harada N, Tamai Y, Ishikawa T, Sauer B, Takaku K, Oshima M, et al. Intestinal polyposis in mice with a dominant stable mutation of the beta-catenin gene. *EMBO J* 1999;18:5931–42.
- Haupt A, Thamer C, Heni M, Ketterer C, Machann J, Schick F, et al. Gene variants of TCF7L2 influence weight loss and body composition during lifestyle intervention in a population at risk for type 2 diabetes. *Diabetes* 2010;59:747–50.
- Kaushal GS, Rognoni E, Lichtenberger BM, Driskell RR, Kretzschmar K, Hoste E, et al. Fate of prominin-1 expressing dermal papilla cells during homeostasis, woundhealing and Wnt activation. *J Invest Dermatol* 2015;135:2926–34.
- Kennell JA, MacDougald OA. Wnt signaling inhibits adipogenesis through beta-catenin-dependent and -independent mechanisms. *J Biol Chem* 2005;280:24004–10.
- Kretzschmar K, Watt FM. Markers of epidermal stem cell subpopulations in adult mammalian skin. *Cold Spring Harb Perspect Med* 2014;4:a013631.
- Lichtenberger BM, Mastrogiannaki M, Watt FM. Epidermal β-catenin activation remodels the dermis via paracrine signalling to distinct fibroblast lineages. *Nat Commun* 2016;7:10537.
- Lim X, Nusse R. Wnt signaling in skin development, homeostasis, and disease. *Cold Spring Harb Perspect Biol* 2013;5:a008029.
- Liu S, Heralut Y, Pavlovic G, Leask A. Skin progenitor cells contribute to bleomycin-induced skin fibrosis. *Arthritis Rheumatol* 2014;66:707–13.
- Longo KA, Wright WS, Kang S, Gerin I, Chiang SH, Lucas PC, et al. Wnt10b inhibits development of white and brown adipose tissues. *J Biol Chem* 2004;279:35503–9.
- Marangoni RG, Korman BD, Wei J, Wood TA, Graham LV, Whitfield ML, et al. Myofibroblasts in murine cutaneous fibrosis originate from adiponectin-positive intradermal progenitors. *Arthritis Rheumatol* 2015;67:1062–73.
- Millar SE. Molecular mechanisms regulating hair follicle development. *J Invest Dermatol* 2002;118:216–25.
- Muller-Rover S, Handjiski B, van der Veen C, Eichmuller S, Foitzik K, McKay IA, et al. A comprehensive guide for the accurate classification of murine hair follicles in distinct hair cycle stages. *J Invest Dermatol* 2001;117:3–15.
- Ohgo S, Hasegawa S, Hasebe Y, Mizutani H, Nakata S, Akamatsu H. Bleomycin inhibits adipogenesis and accelerates fibrosis in the subcutaneous adipose layer through TGF-beta1. *Exp Dermatol* 2013;22:769–71.
- Ohtola J, Myers J, Akhtar-Zaidi B, Zuzindlak D, Sandesara P, Yeh K, et al. Beta-catenin has sequential roles in the survival and specification of ventral dermis. *Development* 2008;135:2321–9.
- Paus R, Muller-Rover S, Van Der Veen C, Maurer M, Eichmuller S, Ling G, et al. A comprehensive guide for the recognition and classification of distinct stages of hair follicle morphogenesis. *J Invest Dermatol* 1999;113:523–32.

Plikus MV, Chuong CM. Macroenvironmental regulation of hair cycling and collective regenerative behavior. *Cold Spring Harb Perspect Med* 2014;4:a015198.

Plikus MV, Mayer JA, de la Cruz D, Baker RE, Maini PK, Maxson R, et al. Cyclic dermal BMP signalling regulates stem cell activation during hair regeneration. *Nature* 2008;451:340–4.

Rinkevich Y, Walmsley GG, Hu MS, Maan ZN, Newman AM, Drukker M, et al. Skin fibrosis. Identification and isolation of a dermal lineage with intrinsic fibrogenic potential. *Science* 2015;348:aaa2151.

Rivers LE, Young KM, Rizzi M, Jamen F, Psachoulia K, Wade A, et al. PDGFRA/NG2 glia generate myelinating oligodendrocytes and piriform projection neurons in adult mice. *Nat Neurosci* 2008;11:1392–401.

Sennett R, Rendl M. Mesenchymal-epithelial interactions during hair follicle morphogenesis and cycling. *Semin Cell Dev Biol* 2012;23:917–27.

Tsai SY, Sennett R, Rezza A, Clavel C, Grisanti L, Zemla R, et al. Wnt/β-catenin signaling in dermal condensates is required for hair follicle formation. *Dev Biol* 2014;385:179–88.

Uezumi A, Fukada S, Yamamoto N, Takeda S, Tsuchida K. Mesenchymal progenitors distinct from satellite cells contribute to ectopic fat cell formation in skeletal muscle. *Nat Cell Biol* 2010;12:143–52.

Zhu AJ, Watt FM. Beta-catenin signalling modulates proliferative potential of human epidermal keratinocytes independently of intercellular adhesion. *Development* 1999;126:2285–98.



This work is licensed under a Creative Commons Attribution 4.0 International License. To view a copy of this license, visit <http://creativecommons.org/licenses/by/4.0/>